Journal of Organometallic Chemistry, 370 (1989) 155–171
Elsevier Sequoia S.A., Lausanne – Printed in The Netherlands
JOM 09743

Resolution of the chiral η^6-methyl-*o*-toluate complex $[RuCl_2(\eta^6\text{-}o\text{-}MeC_6H_4CO_2Me)]_2$. Crystal structure and absolute configuration of the (+)-neomenthyldiphenylphosphine (NMDPP) complex $RuCl_2(\eta^6\text{-}o\text{-}MeC_6H_4CO_2Me)$-[(+)-NMDPP]

Piero Salvadori *, Paolo Pertici, Fabio Marchetti, Raffaello Lazzaroni, Giovanni Vitulli

Centro di Studio del CNR per le Macromolecole Stereordinate ed Otticamente Attive, Dipartimento di Chimica e Chimica Industriale, University of Pisa, via Risorgimento 35, 56100 Pisa (Italy)

and Martin A. Bennett

Research School of Chemistry, Australian National University, G.P.O. Box 4, Canberra, A.C.T. 2601 (Australia)

(Received November 3rd, 1988)

Abstract

The planar chiral η^6-methyl-*o*-toluate-ruthenium(II) complex $[RuCl_2(\eta^6\text{-}o\text{-}MeC_6H_4CO_2Me)]_2$ (**1**) was found to react with (+)-neomenthyldiphenylphosphine (NMDPP) (**2**) to give monomeric diastereomers $[RuCl_2(\eta^6\text{-}o\text{-}MeC_6H_4CO_2Me)$-(NMDPP)] (**3a** and **3b**), which were separated by fractional crystallization. Crystals of the less soluble diastereomer **3a** belong to the space group $P2_12_12_1$, with a 11.998(3), b 16.178(4), c 17.171(4) Å, $Z = 4$, at 293 K. The structure has been solved by Patterson and Fourier techniques and refined by full-matrix least squares analysis to $R = 0.0607$, $R_w = 0.0624$ for 1398 unique reflections with $F_o > 2\sigma(F_o)$. The ruthenium atom is pseudo-octahedrally coordinated by η^6-methyl-*o*-toluate, NMDPP and two chloride ligands (Ru–P 2.357(5), Ru–Cl 2.423(6), 2.381(6) Å). The arene ring is planar within experimental error but it is coordinated unsymmetrically: the Ru–C distances to the unsubstituted carbon atoms are 2.11(3)–2.17(2) Å, whereas those to the carbon atoms bearing the methoxycarbonyl and methyl groups are 2.26(2) Å and 2.30(2) Å, respectively. The absolute configuration at the chiral planar centre of **3a** is *R*. **3a** and **3b** have been converted into (*R*)- and (*S*)-$Ru(\eta^6\text{-}o\text{-}MeC_6H_4CO_2Me)(\eta^4$-1,5-cyclooctadiene) (**6a** and **6b** respectively), from which the (*R*,*R*)- and (*S*,*S*)-$[RuCl_2(\eta^6\text{-}o\text{-}MeC_6H_4CO_2Me)]_2$ have been obtained in enantiomeric purities of 90 and 60%, respectively.

0022-328X/89/$03.50

Introduction

Chiral organometallic complexes have attracted interest recently because they offer the possibility of highly enantioselective catalytic or stoichiometric transformations, some of which are of industrial interest [1–3]. Some organometallic derivatives, such as those derived from $Cr(CO)_3$ attached to optically active steroid hormones, have biochemical applications [4].

We are interested in preparing and resolving arene ruthenium complexes having "planar chirality" [5,6], i.e. complexes containing the unit $Ru(\eta^6\text{-}C_6H_4RR')$, where R, R' are different substituents in 1,2- or 1,3-positions of the arene, since in the optically active form they could be used in asymmetric synthesis. We recently described the methyl-*o*-toluate complex $[RuCl_2(\eta^6\text{-}o\text{-}MeC_6H_4CO_2Me)]_2$ (**1**) and showed that it reacts with optically active amines to give diastereomeric adducts $RuCl_2(\eta^6\text{-}o\text{-}MeC_6H_4CO_2Me)L$ (L = (−)(*S*)-1-phenylethylamine or (+)-dehydroabietylamine) and $[RuCl(\eta^6\text{-}o\text{-}MeC_6H_4CO_2Me)(N\text{-}N)]PF_6$ (N–N = (−)(*R*,*R*)-1,2-diphenyl-1,2-diaminoethane, $PhCH(NH_2)CH(NH_2)Ph$) [7]. Only in the case of the phenylethylamine complex was it possible to achieve a partial separation of the diastereomers by fractional crystallization. Although the less soluble one was obtained with 90% enrichment, the more soluble one could not be obtained in such high optical purity, and the chemical yields were poor. Clearly, a more efficient resolution is needed if compounds of this type are to be used in asymmetric synthesis.

We report here that this problem has been solved, at least in the case of **1**, by use of (+)-neomenthyldiphenylphosphine (NMDPP) (**2**) as resolving agent. **2** forms easily separable diastereomeric adducts with **1** from which the antipodes of **1** can be obtained by removal of coordinated **2**. We also describe an X-ray crystallographic analysis of one of the pure diastereomers, which enables the absolute configuration at the chiral planar centre of **1** to be deduced. The chirooptical properties of the enantiomers **1a** and **1b** are discussed, and the possibility of assigning the absolute configuration to chiral complexes of this type is considered.

Results

Complex **1** reacted with a stoichiometric quantity of **2** in refluxing 2-propanol to give the monomeric complex $RuCl_2(\eta^6\text{-}MeC_6H_4CO_2Me)(NMDPP)$ (**3**) almost quantitatively (Scheme 1). The ^1H NMR spectrum of **3** (Fig. 1a) shows two singlets of equal intensity, at δ 3.93, 3.88 ppm, due to the CO_2Me protons, and two singlets, also of equal intensity, at δ 2.57, 2.32 ppm, due to the aromatic methyl protons. The two sets of peaks arise from diastereomers of **3** present in equal amounts. One crystallization from dichloromethane/ether/hexane (2/2/1) at room temperature gave the less soluble diastereomer **3a** in 40% yield, containing only about 5% of the more soluble diastereomer **3b**. The latter was obtained in ca 80% diastereomeric purity by several recrystallizations from dichloromethane/ether of solid obtained from the mother liquor. Slow crystallization of the 95/5 mixture of **3a**/**3b** from methanol/ether gave single crystals of **3a** in > 99% diastereomeric purity.

The diastereomers could also be distinguished by the chemical shifts of their singlet $^{31}P\{^1H\}$ resonances: δ(P) (relative to external 85% H_3PO_4) 42.2 and 40.2 for **3a** and **3b**, respectively.

The ^1H NMR spectrum of pure **3a** is shown in Fig. 1(b). The proton resonances of the complexed aromatic ring appear as four multiplets in the region δ 6.2–3.3

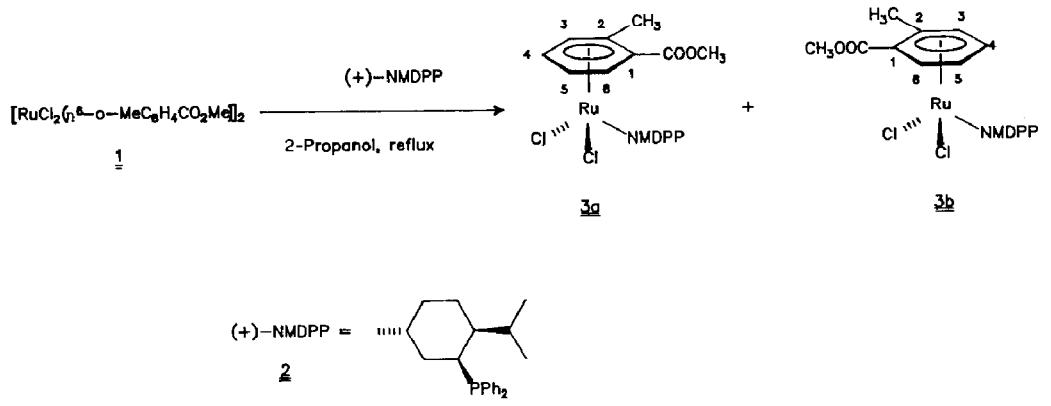

Scheme 1

ppm, and thus span a remarkably large range (2.9 ppm). The resonance at δ 6.13 ppm is assigned to H6, *ortho* to the deshielding group CO_2Me, by analogy with the spectral assignments for **1** and its derivatives [7], and for $Cr(CO)_3(\eta^6$-*o*-$MeC_6H_4CO_2Me)$ [8]. The resonance at δ 3.3 ppm is assigned to H5, *meta* to the CO_2Me group. The X-ray study of **3a** (see below) suggests that the unexpected shielding of H5 may arise from a preference in solution for a rotamer in which this proton lies in the shielding zone of one of the phenyl rings of coordinated NMDPP.

The absorption and circular dichroism (CD) spectra of pure **3a** and of a 20/80 diastereomeric mixture of **3a** and **3b** are shown in Fig. 2(a) and 2(b). In the absorption spectrum two different regions can be easily distinguished on intensity grounds: the first relates to the spectral range down to 300 nm, and the second to the 300–200 nm range. In the former range there is an absorption maximum at ca. 360 nm, with a strong tail up to 550 nm, while two bands having opposite signs can be clearly seen in the CD spectrum around 500 and 380 nm. When account is taken of the intensity of the bands in ordinary absorption, it seems that the spectral region down to 450 nm may be related to *d–d* transitions located on the metal, whilst the absorptions in the range 450–300 nm can be regarded as arising from charge transfer transitions. The 300–200 nm region, in which strong absorption bands are measured, is certainly dominated by internal ligand transitions and/or charge transfer promotions.

X-Ray structural analysis of $RuCl_2(\eta^6$-*o*-$MeC_6H_4CO_2Me)$*(NMDPP)* · *MeOH (3a)*

The molecular structure is shown in Fig. 3, and the coordination sphere of the ruthenium atom is shown in more detail in Fig. 4. Important bond distances and angles are in Table 1. In terms of the *R,S* system as extended to complexes having planar chirality [9], the absolute configuration of the chiral planar centre in **3a** is *R*.

The crystal lattice contains one molecule of clathrate methanol for each molecule of **3a**. The coordination geometry about the ruthenium atom can be described as distorted octahedral, with the arene occupying three facial coordination sites. The angles between the monodentate ligands are close to 90° (Cl1–Ru–Cl2 88.3°, Cl1–Ru–P 88.7°, Cl2–Ru–P 89.9°). The arene ring and the three other ligands are mutually staggered, as in the closely related complexes $RuCl_2(\eta^6$-$C_6H_6)(PMePh_2)$ (**4**) and $RuCl_2(\eta^6$-*p*-$MeC_6H_4CHMe_2)(PMePh_2)$ (**5**) [10].

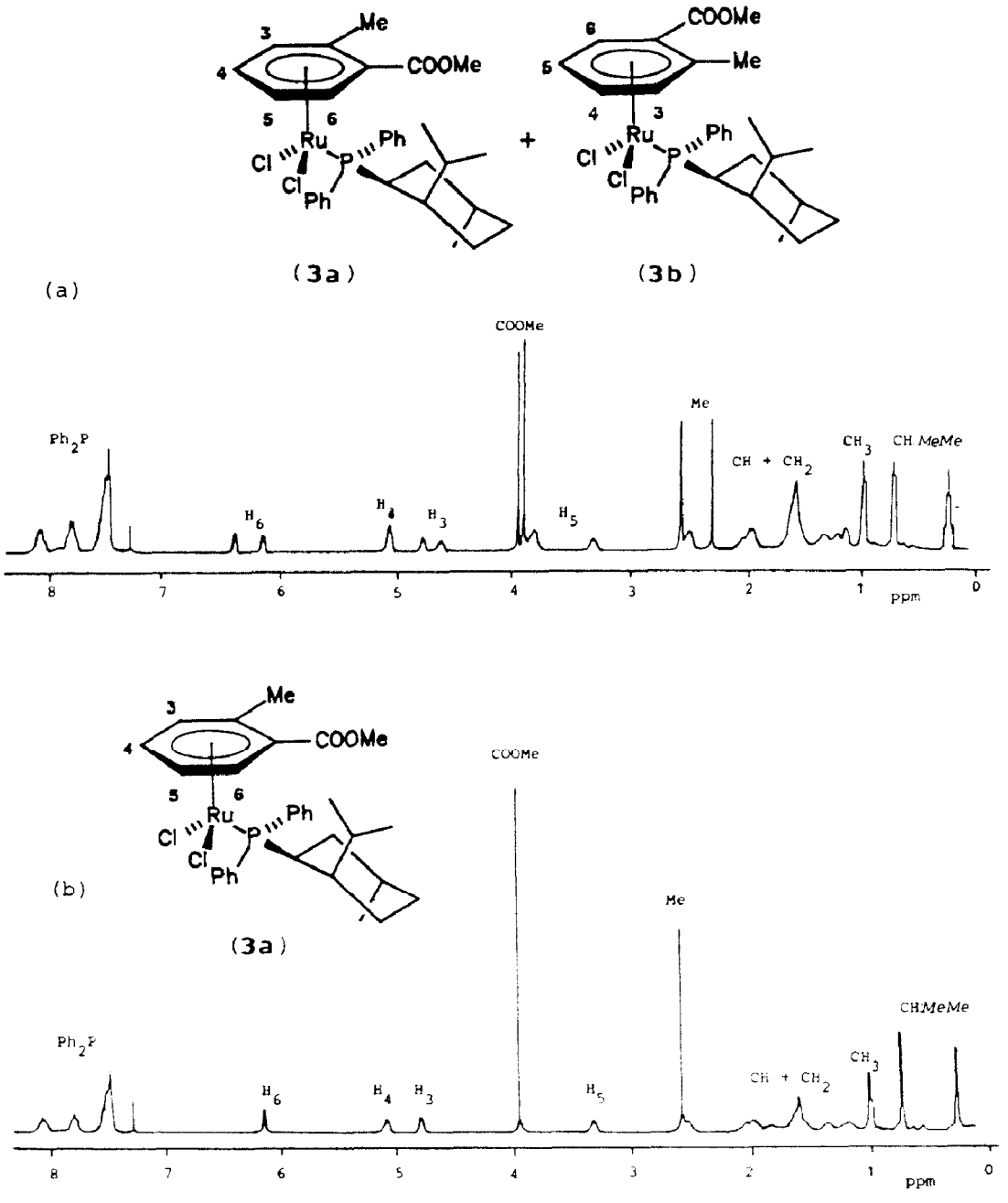

Fig. 1. ^{1}H NMR spectra (300 MHz, $CDCl_3$) of: (a) 1/1 mixture of the two diastereomers [$RuCl_2(\eta^6$-*o*-$MeC_6H_4CO_2Me$)(NMDPP)] (**3a** and **3b**); (b) pure **3a**.

A common feature of **3a**, **4** and **5** is the unsymmetrical attachment of the arene ring to the ruthenium atom. In **3a** the Ru–C distances to the unsubstituted carbon atoms C2, C3, C4 and C5 * are in the range 2.11(3)–2.17(2) Å, whereas those to C1

* Note that the crystallographic numbering system for **3a** differs from that used in discussing the NMR spectra.

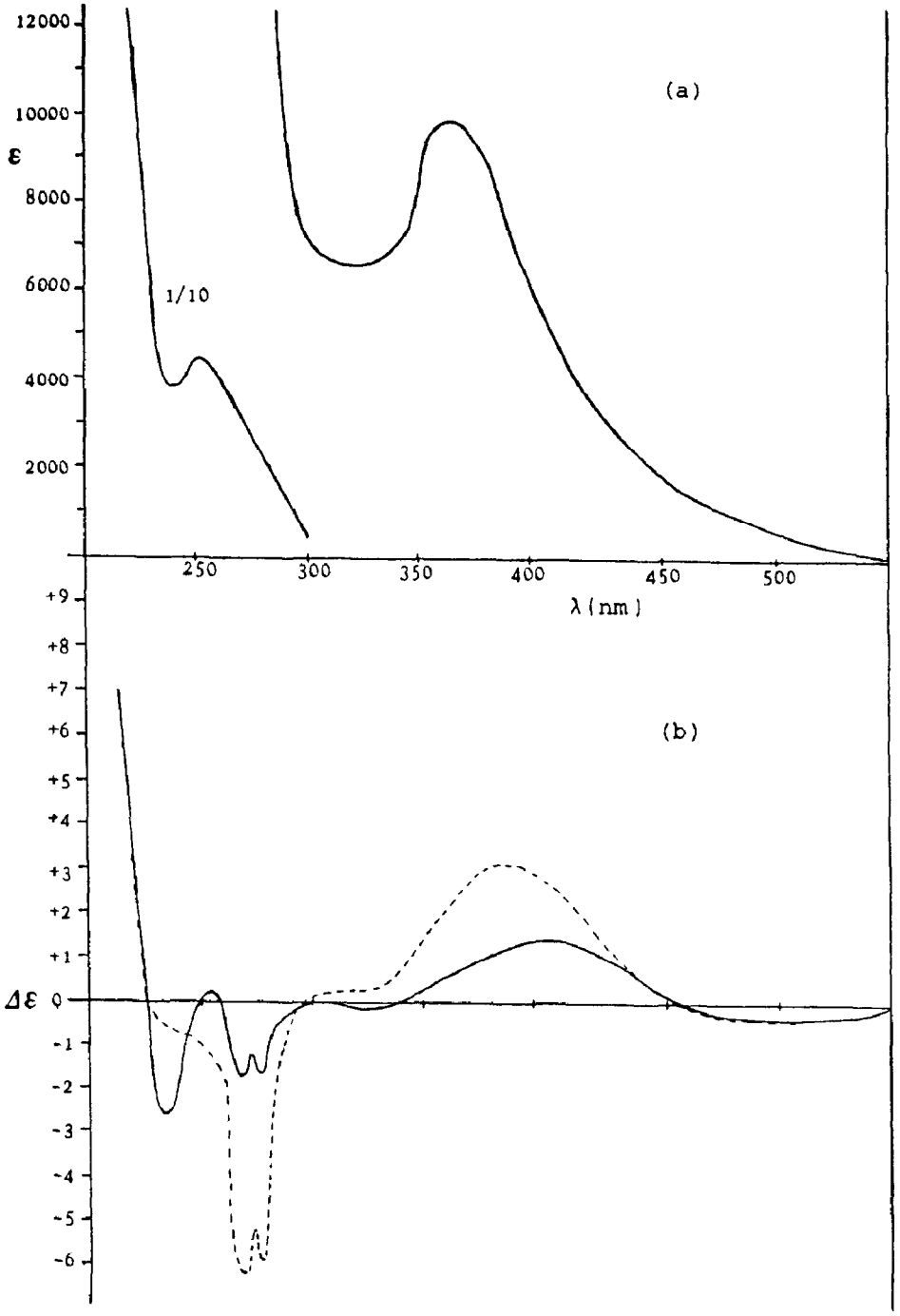

Fig. 2. (a) UV and (b) CD spectra (c 2×10^{-3} mol dm^{-3}, MeCN) of the diastereomers [$RuCl_2(\eta^6$-*o*-$MeC_6H_4CO_2Me$)(NMDPP)] (**3a** and **3b**). (———) **3a**; (— — —) **3a**/**3b** 20/80.

and C6, which bear the methoxycarbonyl and methyl groups, are 2.26(2) and 2.30(2) Å, respectively.

Similar values have been reported for **4** and **5** [10]. In all cases the longer bonds are *trans* to the tertiary phosphine, which has a higher *trans*-influence than chloride.

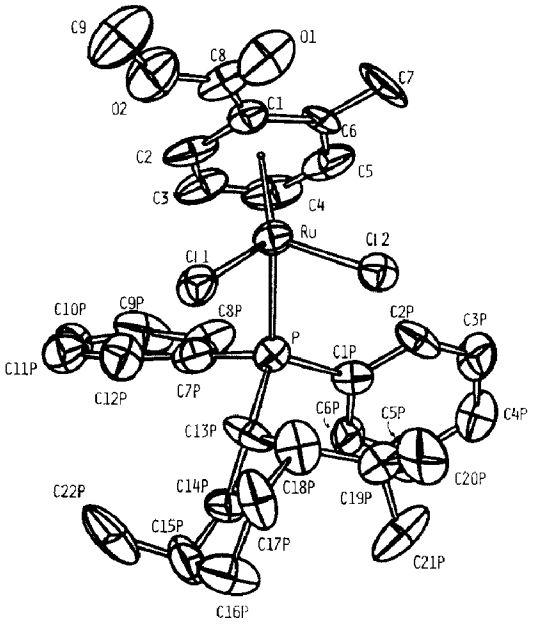

Fig. 3. Molecular structure of the complex [$RuCl_2(\eta^6$-*o*-$MeC_6H_4CO_2Me$)(NMDPP)] (**3a**).

The arene ring in **3a** is essentially planar, the maximum out-of-plane displacement being only 0.02(2) Å, which is within the standard deviation. The dihedral angle of 1.9° between the plane C2–C1–C6–C5 and C2–C3–C4–C5 is similar to that reported for the *p*-cymene complex **5** (2°), but is significantly smaller than that for the benzene complex **4** (5°) in which the ring is clearly not quite planar. The C–C bond lengths in the ring are in the range 1.31(4)–1.44(3) Å, with a mean value of 1.39 Å.

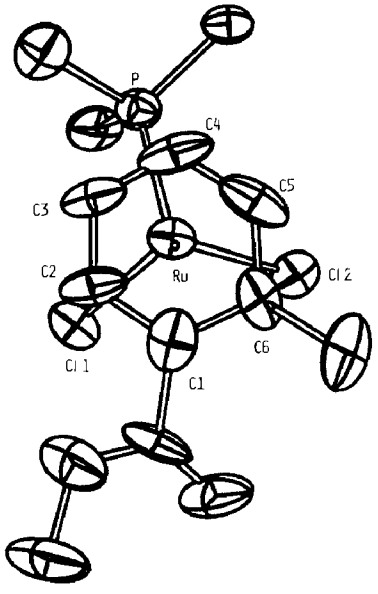

Fig. 4. A view of the coordination sphere around the ruthenium atom in the complex **3a**.

Table 1

Bond distances (Å) and angles (degrees) in the complex **3a**. Esd's are given in parentheses (Car = centroid of the arene).

Ru–Cl1	2.420(6)	C2–C3	1.34(4)	C8p–C9p	1.37(4)
Ru–Cl2	2.381(6)	C3–C4	1.41(4)	C9p–C10p	1.37(4)
Ru–P	2.357(6)	C4–C5	1.31(4)	C10p–C11p	1.34(5)
Ru–C1	2.26(2)	C5–C6	1.44(3)	C11p–C12p	1.31(4)
Ru–C2	2.17(2)	C6–C7	1.51(3)	C13p–C14p	1.53(3)
Ru–C3	2.15(3)	O1–C8	1.18(4)	C13p–C18p	1.53(4)
Ru–C4	2.11(3)	O2–C8	1.31(4)	C14p–C15p	1.45(4)
Ru–C5	2.13(3)	O2–C9	1.49(4)	C15p–C16p	1.59(5)
Ru–C6	2.30(2)	C1p–C2p	1.39(3)	C15p–C22p	1.49(5)
Ru–Car	1.69(3)	C1p–C6p	1.40(3)	C16p–C17p	1.63(4)
P–C1p	1.82(2)	C2p–C3p	1.37(4)	C17p–C18p	1.50(3)
P–C7p	1.85(3)	C3p–C4p	1.40(4)	C18p–C19p	1.54(4)
P–C13p	1.87(3)	C4p–C5p	1.36(4)	C19p–C20p	1.49(4)
C1–C2	1.41(4)	C5p–C6p	1.46(4)	C19p–C21p	1.53(4)
C1–C6	1.41(3)	C7p–C8p	1.43(4)	Om–Cm	1.29(8)
C1–C8	1.54(3)	C7p–C12p	1.40(4)		

Cl1–Ru–Cl2	88.3(2)	C1p–C2p–C3p	120.0(2)
Cl1–Ru–P	88.7(2)	C2p–C3p–C4p	123.0(2)
Cl1–Ru–Car	125.5(9)	C3p–C4p–C5p	118.0(2)
Cl2–Ru–P	89.8(2)	C4p–C5p–C6p	120.0(3)
Cl2–Ru–Car	125.0(1)	C5p–C6p–C1p	120.0(2)
P–Ru–Car	127.2(9)	P–C7p–C8p	121.0(2)
C2–C1–C6	120.0(2)	PC7p–C12p	120.0(2)
C2–C1–C8	115.0(2)	C8p–C7p–C12p	118.0(2)
C6–C1–C8	125.0(2)	C7p–C8p–C9p	114.0(2)
C1–C2–C3	123.0(2)	C8p–C9p–C10p	127.0(3)
C2–C3–C4	118.0(3)	C9p–C10p–C11p	115.0(3)
C3–C4–C5	119.0(3)	C10p–C11p–C12p	123.0(3)
C4–C5–C6	126.0(3)	C11p–C12p–C7p	122.0(3)
C5–C6–C1	113.0(2)	P–C13p–C14p	115.0(2)
C5–C6–C7	125.0(2)	P–C13p–C18p	117.0(2)
C1–C6–C7	122.0(2)	C14p–C13p–C18p	114.0(2)
C1–C8–O1	123.0(2)	C13p–C14p–C15p	117.0(2)
C1–C8–O2	112.0(2)	C14p–C15p–C16p	110.0(2)
O1–C8–O2	125.0(2)	C14p–C15p–C22p	112.0(3)
C8–O2–C9	119.0(3)	C16p–C15p–C22p	107.0(3)
Ru–P–C1p	115.9(8)	C15p–C16p–C17p	112.0(2)
Ru–P–C7p	107.5(9)	C16p–C17p–C18p	115.0(2)
Ru–P–C13p	116.9(9)	C17p–C18p–C13p	107.0(2)
C1p–P–C7p	104.0(1)	C17p–C18p–C19p	117.0(2)
C1p–P–C13p	109.0(1)	C13p–C18p–C19p	118.0(2)
C7p–P–C13p	102.0(1)	C18p–C19p–C20p	111.0(2)
P–C1p–C2p	122.0(2)	C18p–C19p–C21p	118.0(2)
P–C1p–C6p	119.0(2)	C20p–C19p–C21p	109.0(2)
C2p–C1p–C6p	119.0(2)		

The mean value of the Ru–C bond lengths in **3a** (2.18 Å) is close to those in **4** and **5** (2.21, 2.23 Å, respectively). The Ru–Cl distances in **3a** (2.423(6), 2.381(6) Å) also agree well with the corresponding bond lengths in **4** and **5** (2.41 Å, av.). The fact that the Ru–P bond length in **3a** (2.353(5) Å) is slightly greater than those in **4**

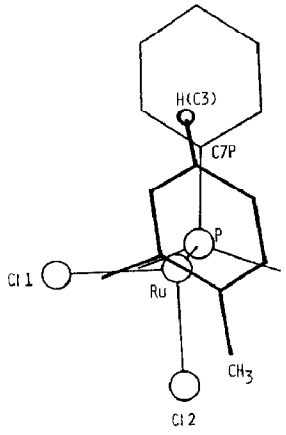

Fig. 5. A view of the complex **3a**, showing the position of the hydrogen atom H3 on C3 of the η^6-arene with respect to the phosphine phenyl ring C7...C12.

and **5** (2.336, 2.341 Å, respectively) is probably a consequence of the greater bulk of NMDPP relative to $PMePh_2$. Although no crystal structures of complexes of NMDPP seem to have been reported, the bond distances and angles in the neomenthyl fragment of **3a** are similar to those found in nickel(II) and palladium(II) complexes of neomenthyldimethylphosphine [11].

One of the phenyl rings of the coordinated NMDPP in **3a** is close to the coordinated methyl-*ortho*-toluate. As shown in Fig. 5, the hydrogen atom H3 on C3 of the η^6-arene points towards the phosphine phenyl ring C7p.....C12p. The distance between H3 and the centre of the ring is only 2.63(3) Å, and the angle between the ring plane and the line containing H3 and the centre of the ring is 73°, i.e. not far from 90°. These values are consistent with the suggestion that H3 (corresponding to H5 in the NMR notation, see above) is in the shielding zone of the phenyl ring C7p.....C12p.

*Enantiomers of Ru(η^6-o-$MeC_6H_4CO_2Me$)(COD) (**6**) and [$RuCl_2$(η^6-o-$MeC_6H_4CO_2$-Me)] (**1**)*

Coordinated NMDPP was removed from the diastereomers (*R*)-**3a** (95% enriched) and (*S*)-**3b** (80% enriched) by heating them with 1,5-cyclooctadiene (COD) in the presence of 2-propanol and anhydrous sodium carbonate, following our recently described procedure [12]. The corresponding enantiomers (*R*)-**6a** and (*S*)-**6b** of the zerovalent ruthenium complex Ru(η^6-o-$MeC_6H_4CO_2Me$)(COD) were obtained (Scheme 2).

$$\underset{(\mathbf{3a}/\mathbf{3b})}{RuCl_2(\eta^6\text{-}o\text{-}MeC_6H_4CO_2Me)(NMDPP)} + COD + (CH_3)_2CHOH + Na_2CO_3 \xrightarrow{\Delta}$$

$$\underset{(\mathbf{6a}/\mathbf{6b})}{Ru(\eta^6\text{-}o\text{-}MeC_6H_4CO_2Me)(COD)} + (CH_3)_2CO + NMDPP + 2NaCl + H_2O + CO_2$$

Scheme 2

The yields were ca. 45% after chromatography on alumina and elution with hexane. Toluene eluted the displaced NMDPP, the recovery being ca. 50%. As expected, the CD spectra of (*R*)-**6a** and (*S*)-**6b** (Fig. 6) are mirror images, the difference in intensity being due to the different optical purities.

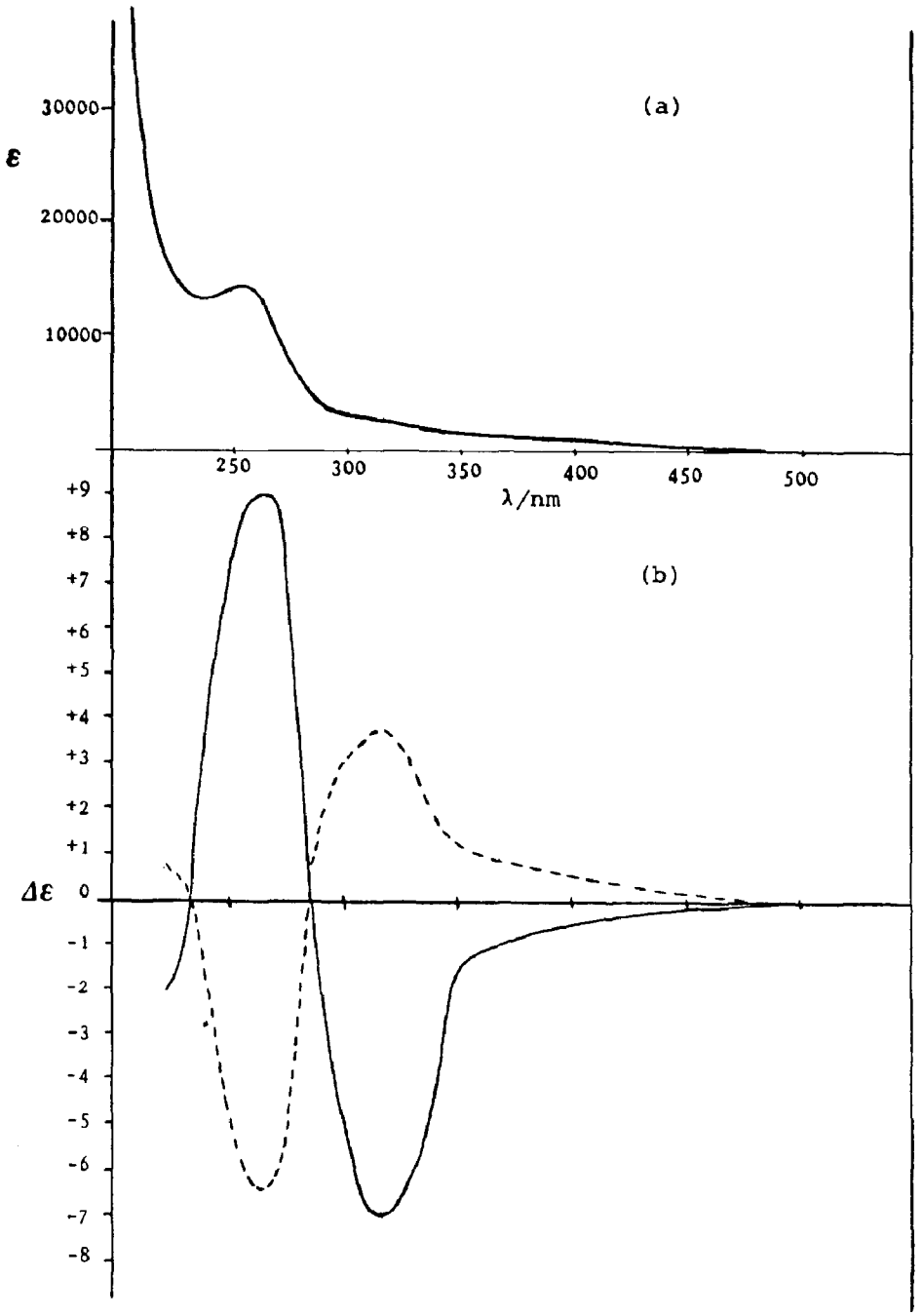

Fig. 6. (a) UV and (b) CD spectra (c 2×10^{-3} mol dm^{-3}, n-pentane) of the enantiomers (−)(*R*)-Ru(η^6-*o*-$MeC_6H_4CO_2Me$)(COD) (**6a**), 90% e.e. (———) and (+)(*S*)-Ru(η^6-*o*-$MeC_6H_4CO_2Me$)(COD) (**6b**), 60% e.e. (— — —).

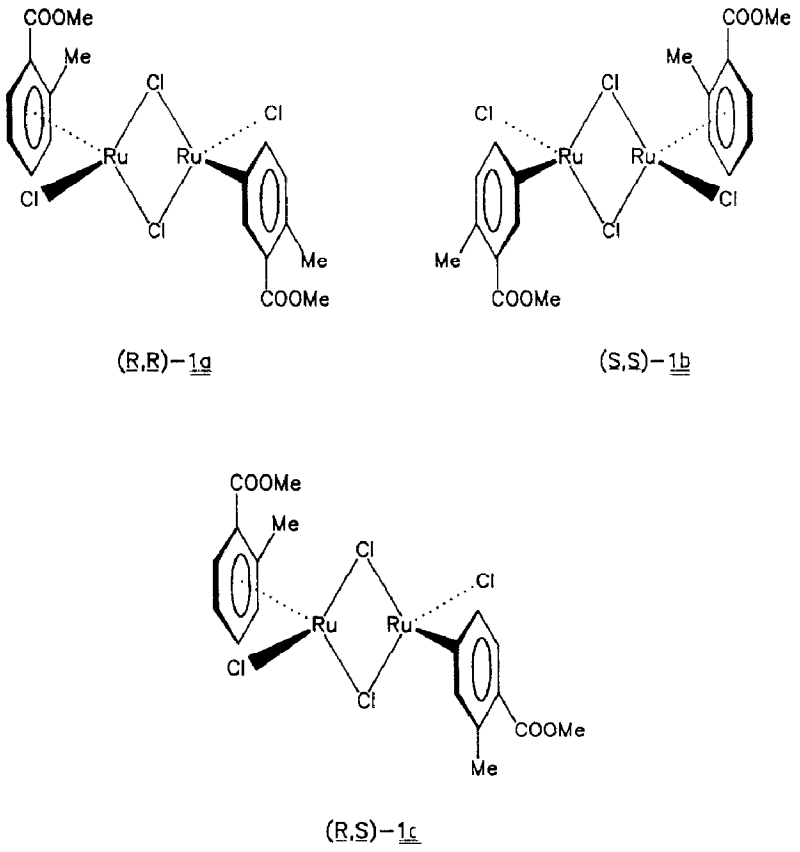

Fig. 7. Stereoisomers of the complex $[RuCl_2(\eta^6\text{-}o\text{-}MeC_6H_4CO_2Me)]$ (**1**).

The COD complexes (*R*)-**6a** and (*S*)-**6b** were separately treated with concentrated HCl in acetone [13] to give the antipodes of the dimeric chloro-bridged complexes $[RuCl_2(\eta^6\text{-}o\text{-}MeC_6H_4CO_2Me)]_2$, (*R*,*R*)-**1a** and (*S*,*S*)-**1b**, respectively. The enantiomeric purities of the samples of **6a** and **6b** used in this experiment were 90 and 60%, respectively, so in both cases some of the *meso*-form of the dimer, (*R*,*S*)-**1c** could have been formed (Fig. 7). In acetonitrile solution, however, in which the optical rotatory power and circular dichroism were measured, **1a** and **1b** exist as monomeric solvento complexes $RuCl_2(\eta^6\text{-}o\text{-}MeC_6H_4CO_2Me)(NCMe)$ [7] whose enantiomeric purity corresponds with that of the precursors **6a** and **6b**. The CD spectra of **1a** (90% enantiomeric purity) and **1b** (60% enantiomeric purity) shown in Fig. 8 are mirror images, the corresponding optical rotations being -32 and $+24°$ (*c* 0.1, acetonitrile), respectively.

Discussion

Many planar chiral metallocene and arene tricarbonylchromium complexes containing carboxylic acid or carbonyl functions have been resolved by traditional organic methods, e.g. separation of diastereomeric menthyl esters [14]. As far as we are aware, the present report describes the first resolution of a planar chiral arene ruthenium(II) complex. As previously reported [7], the traditional methods of

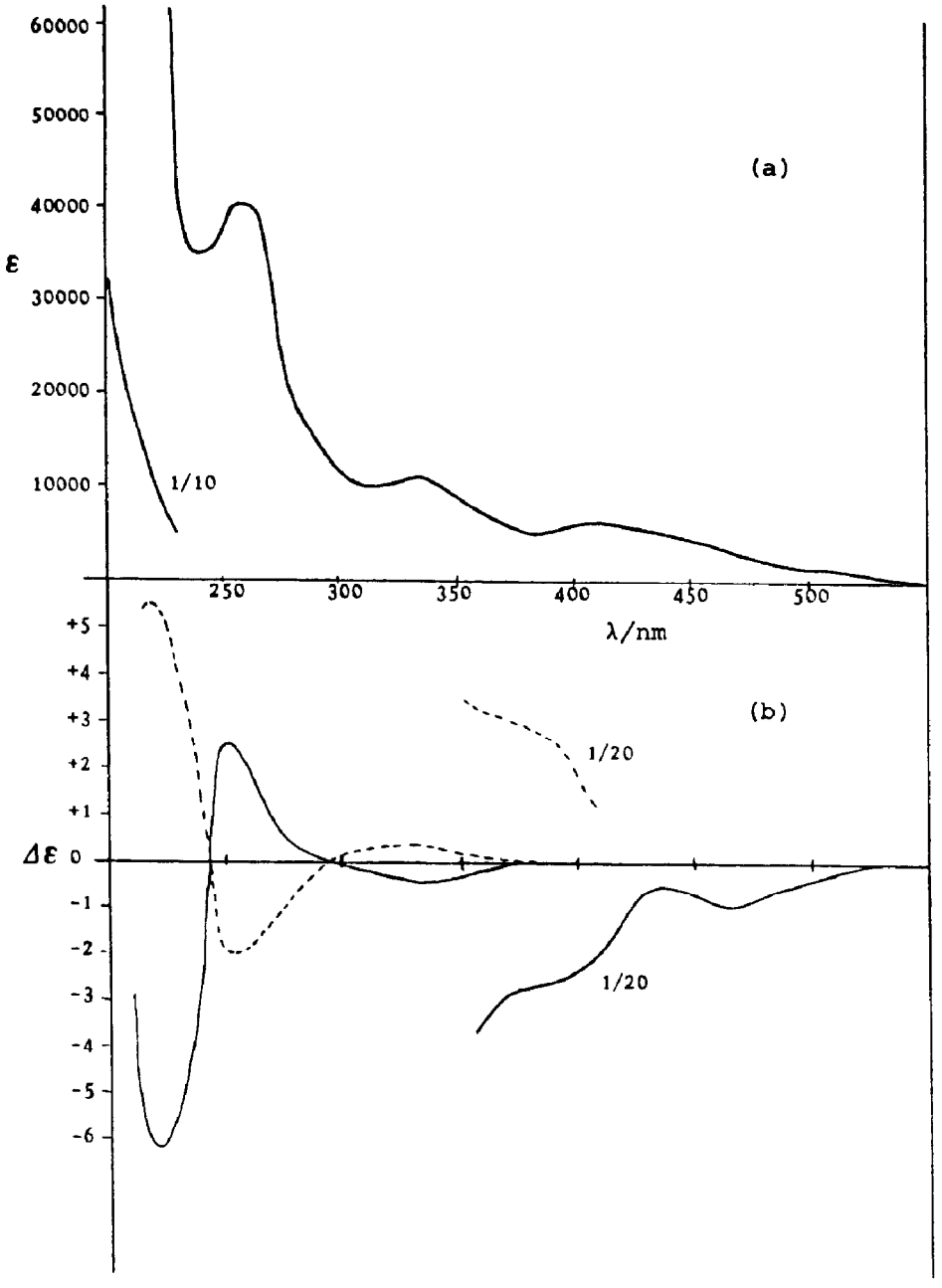

Fig. 8. (a) UV and (b) CD spectra ($c\ 1\times10^{-3}$ mol dm^{-3}, MeCN) of the enantiomers (−)(*R*)-$RuCl_2(\eta^6$-*o*-$MeC_6H_4CO_2Me)$(NCMe) (**1a**), 90% e.e. (———) and (−)(*S*)-$RuCl_2(\eta^6$-*o*-$MeC_6H_4CO_2Me)$(NCMe) (**1b**), 60% e.e. (— — —).

resolution failed in the case of $[RuCl_2(\eta^6$-*o*-$MeC_6H_4CO_2Me)]_2$; it was necessary first to bind the resolving agent to the metal atom and subsequently to remove it. The method we have used should be applicable also to the resolution of other chiral $[RuCl_2(\eta^6$-arene$)]_2$ complexes. Related η^6-arene compounds in which the metal atom is the chiral centre have been obtained as diastereomers, viz. $RuClMe(\eta^6$-$C_6H_6)\{Ph_2PNHCH(Me)Ph\}$ [15] and $RuCl(\eta^6$-$C_6H_6)\{NH_2CH(Me)COO\}$ [16].

The diastereomers $RuCl_2(\eta^6\text{-}o\text{-}MeC_6H_4CO_2Me)L$ formed with L = NMDPP differ much more in solubility, and so are more easily separated than those with L = (−)(*S*)-1-phenylethylamine or (+)-dehydroabietylamine [7]. This provides another example of the easy separation of diastereomers containing optically active phenylphosphines as ligands, cf. $RuClMe(\eta^6\text{-}C_6H_6)\{Ph_2PNHCH(Me)Ph\}$ [15] and $RuCl(\eta^5\text{-}C_5H_5)\{Ph_2PCH(R)CH_2PPh_2\}$ (R = Me, cyclo-C_6H_{11}, Ph) [17]. Although the resolving agent NMDPP is fairly expensive, it can be recovered in 50% yield.

The reaction of **3a** and **3b** with Na_2CO_3/2-propanol/1,5-cyclooctadiene to give **6a**, **6b** (Scheme 2), and the reaction of **6a**, **6b** with HCl to give **1a**, **1b**, both occur with retention of configuration at the planar chiral centre. Reaction of **1a** (or **1b**) with NMDPP gives the initial adduct **3a** (or **3b**) with the same optical purity. Thus, since the absolute configuration at the planar chiral centre of diastereomer **3a** is known from X-ray crystallography, the absolute configurations of the enantiomers **6a**, **6b** and **1a**, **1b** can be assigned.

It is not possible to assign the observed transition in the absorption and c.d. spectra of the enantiomers **6a**, **6b** and **1a**, **1b** (Fig. 6 and 8), even when account is taken of reports in the literature on specific spectroscopic studies of arene-ruthenium-(0) and -(II) derivatives; however, some interesting information can be extracted. First, the mirror image relationship between the curves corresponding to **6a**, **6b** and **1a**, **1b** is clear evidence that the enantiomers of **6** and **1** have been obtained; the difference in intensity is attributed to a different enantiomeric composition of the two samples. Second, since the absolute configuration of the planar chiral centre has been determined by means of X-ray analysis and the reactions employed in the transformation **3** → **6** → **1** are completely stereospecific, the CD spectra also represent a powerful tool for configurational assignments for these families of compounds. In other words, the absolute configuration of different chiral $\eta^6\text{-}C_6H_4RR'$ complexes of Ru^0 and Ru^{II}, where the R and R′ substituents of the arene ligand are groups which do not greatly affect the spectroscopic properties of the complexes with respect to those of the parent compounds **6** and **1**, can be determined by recording the CD spectrum and observing the sign sequences of the bands measured. For instance, the (*S*)-absolute configuration in complex **6** can be related to a positive CD band at 330 nm.

The UV and CD spectra of the enantiomers **1a** and **1b** did not change significantly when solutions in acetonitrile or dimethylsulphoxide were kept at 80 °C for 24 h. At higher temperatures some decomposition occurred, but the UV and CD spectra did not change. This configurational stability should prove to be an important advantage in possible application of these compounds as catalyst precursors in asymmetric synthesis.

Experimental

Complex **3** was prepared under dry oxygen-free nitrogen by use of conventional Schlenk-tube techniques; it is air-stable as a solid once isolated. Solvents were dried and degassed before use. The complex $[RuCl_2(\eta^6\text{-}o\text{-}MeC_6H_4CO_2Me)]_2$ (**1**) was prepared as already described [7]. A commercial sample of (+)-neomenthyldiphenylphosphine (NMDPP, **2**) was used as received.

^1H and ^{31}P NMR spectra were recorded on a Varian XR 300 instrument at 300 MHz and 121 MHz, respectively. Proton chemical shifts were determined relative to

internal $(CH_3)_4Si$ (δ 0 ppm), and ^{31}P chemical shifts (δ(P)) relative to 85% H_3PO_4 (positive to high frequency). Coupling constants J are in Hz; the aromatic protons of methyl-*o*-toluate are numbered as shown in Scheme 1. Circular dichroism spectra were recorded for acetonitrile solutions on a Jasco J-500 dichrograph. Ultraviolet and visible spectra in the same solvent were recorded on a Jasco UVIDEL 710 spectrometer. Microanalyses were carried out by the Istituto di Chimica Organica, Facoltà di Farmacia, Università di Pisa, Italy.

*Preparation of dichloro(η^6-methyl-o-toluate){(+)-neomenthyldiphenylphosphine}-ruthenium(II), $RuCl_2(\eta^6$-o-$MeC_6H_4CO_2Me)$(NMDPP) (enantiomeric mixture **3a**/**3b**)*

A stirred suspension of **1** (0.5 g, 0.77 mmol) and **2** (0.5 g, 1.54 mmol) in 2-propanol (50 ml) was heated under reflux for 2 h. The red-brown solution was filtered and the solvent was removed in vacuo. The residue was washed several times with ether and sucked dry to give **3** (0.9 g, 1.39 mmol, 90%) as a 1/1 mixture of diastereomers **3a** and **3b**, as estimated from the intensity ratio of the singlets due to the CO_2Me protons at δ 3.93, 3.88 ppm (Fig. 1(a)) (Found: C, 57.35; H, 6.4; Cl, 10.5; P, 4.95. $C_{31}H_{39}Cl_2O_2PRu$ calcd.: C, 57.58; H, 6.08; Cl, 10.96; P, 4.79%.

Two crystallizations from dichloromethane/ether (1/2) or dichloromethane/ether/hexane (2/2/1) gave the less soluble diastereomer **3a** of ca. 95% purity as an orange-red solid (0.36 g, 40%). ^1H NMR (δ, $CDCl_3$): 8.1, 7.8, 7.45 (m, 2H, 2H, 6H, Ph), 6.13 (d, 1H, J 5.8, H6), 5.07 (m, 1H, H4), 4.78 (m, 1H, H3), 3.93 (s, 3H, CO_2Me), 3.3 (m, 1H, H5), 2.57 (s, 3H, C_6H_4Me), 2.55–1.10 (overlapping m, 10H, CH, CH_2 of NMDPP), 0.99 (d, 3H, J 6.5, Me of NMDPP), 0.72 (d, 3H, J 6.6, CH*Me*Me), 0.25 ppm (d, 3H, J 6.6, CHMe*Me*). $^{31}P\{^1H\}$ NMR (δ, $CDCl_3$): 42.2 (s) ppm.

Addition of ether to the mother liquor from the first recrystallization gave a red solid containing 60–75% of the more soluble diastereomer. Further recrystallization from dichloromethane/ether (1/3) gave **3b** (0.2 g, 22%) in ca. 80% enantiomeric purity. ^1H NMR (δ, $CDCl_3$): 8.1, 7.8, 7.45 (m, 2H, 2H, 6H, Ph), 6.36 (d, 1H, J 5.7, H6), 5.07 (m, 1H, H4), 4.61 (m, 1H, H_3), 3.88 (s, 3H, CO_2 Me), 3.82 (m, 1H, H_5), 2.32 (s, 3H, C_6H_4Me), 2.55–1.10 (overlapping m, 10H, CH and CH_2 of NMDPP), 0.97 (d, 3H, J 6.5, Me of NMDPP), 0.70 (d, 3H, J 6.6, CH*Me*Me), 0.23 ppm (d, 3H, J 6.6, CHMe*Me*). $^{31}P\{^1H\}$ NMR (δ, $CDCl_3$): 40.2 (s) ppm.

*Conversion of (R)- and (S)-$RuCl_2(\eta^6$-o-$MeC_6H_4CO_2Me)$[(+)-NMDPP] (**3a** and **3b**) into (R)- and (S)-$Ru(\eta^6$-o-$MeC_6H_4CO_2Me)$(COD) (**6a** and **6b**)*

The procedure follows that described previously [12]. A suspension of **3a** (550 mg, 0.851 mmol, enantiomeric purity 95%) and anhydrous Na_2CO_3 (400 mg, 3.77 mmol) in 1,5-cyclooctadiene (3 ml, 24.5 mmol) and 2-propanol (25 ml) was heated under reflux for 3 h. The yellow-brown solution was evaporated to dryness under reduced pressure and the residue was extracted with hexane (4 × 20 ml). The extract was concentrated to 10 ml and chromatographed on an alumina column (20 cm, activity II-III). Hexane eluted a yellow fraction, which on evaporation under reduced pressure gave 132 mg (0.366 mmol, 43%) of (−)(*R*)-Ru(η^6-$MeC_6H_4CO_2Me$)(COD) (**6a**) as a yellow solid having [α] −128° (c = 0.1, n-pentane). Elution with toluene gave a second fraction containing **2** (152 mg, 0.468 mmol, 55% recovery).

Similar treatment of 80% enantiomerically pure **3b** gave (+)(*S*)-Ru(η^6-*o*-$MeC_6H_4CO_2Me$)(COD) (**6b**) having [α] +110° ($c = 0.1$, n-pentane).

*Conversion of (R)- and (S)-Ru(η^6-o-$MeC_6H_4CO_2Me$)(COD) (**6a** and **6b**) into (R,R)- and (S,S)-[$RuCl_2(\eta^6$-o-$MeC_6H_4CO_2Me)$] (**1a** and **1b**)*

In a 10 ml Schlenk tube containing a magnetic stirring bar was placed 90% enantiomerically pure **6a** (80 mg, 0.222 mmol) and acetone (3 ml). The mixture was stirred and treated with 4 ml of a 1/3 mixture of concentrated HCl and acetone, the colour changing immediately to dark red. After 3 h stirring at room temperature the mixture was evaporated to dryness and the residue washed with ether to give **1a** (70 mg, 100% yield) as a red-brown solid having [α] −32° ($c = 0.01$, MeCN). Its ^{1}H NMR spectrum agreed with that reported previously [7].

Table 2

Experimental data for the crystallographic analysis

Compound	**3a**
Formula	$C_{31}H_{39}Cl_2O_2PRu.CH_3OH$
M	720.7
Space group	$P2_12_12_1$
a (Å)	11.998(3)
b (Å)	16.138(4)
c (Å)	17.171(4)
U (Å^3)	3325(1)
Z	4
D_c (Mg m^{-3})	1.440
Radiation	Mo-K_{α_1}
λ (Å)	0.71069
F(000)	1504
T (K)	293
Crystal size (mm)	0.12×0.27×0.56
Diffractometer	Ital Structures
μ (mm^{-1})	0.704
Scan speed (° s^{-1})	0.10
Scan width (°)	1.20
θ-range (°)	3–26
h-range	0–11
k-range	0–19
l-range	0–19
Standard reflection	200,044
Intensity variation	none
Scan mode	$\theta/2\theta$
No. of measured reflections	2115
Condition of observed reflections	$I > 2\sigma(I)$
No. of reflections used in the refinement	1398
Max. least-squares shift-to-error ratio	0.5
Min., Max. height in final Fourier map, ρ (eÅ^{-3})	−0.41/0.80
No. of refined parameters	381
$R = \Sigma\|\Delta F\|/\Sigma\|F_o\|$	0.0615
$R' = [\Sigma w(\Delta F)^2/\Sigma wF_o^2]^{1/2}$	0.0658
w	$k/[\sigma^2(F_o) + 0.0435F_o^2]$

Similar treatment of a 60% enantiomerically pure sample of **6b** gave **1b** having $[\alpha]$ $+24°$ ($c = 0.01$, MeCN).

Crystal structure determination

A crystal suitable for X-ray analysis was obtained from methanol/ether. Details of the lattice parameters, data collection, and structure refinement are summarized in Table 2. The symmetry class and space group were determined from the systematic absences on Weissenberg photographs. The unit cell dimensions and

Table 3

Fractional coordinates ($\times 10^4$) for Ru, Cl and P atoms and ($\times 10^3$) for C and O atoms and isotropic B equivalent (B_{eq} $\frac{1}{3}$ trace of the diagonalized matrix). Esd's are given in parentheses

Atom	x	y	z	B_{eq}
Ru	7030(2)	1686(1)	5323(1)	3.34(6)
Cl1	5525(5)	871(4)	4781(4)	4.4(2)
Cl2	5680(5)	2433(4)	6058(3)	4.1(2)
P	7179(5)	711(4)	6339(3)	3.2(2)
C1	738(2)	241(2)	422(2)	4.8(7)
C2	786(2)	161(2)	420(1)	5.0(7)
C3	855(2)	132(2)	475(2)	5.0(7)
C4	878(2)	184(2)	540(2)	5.4(9)
C5	833(2)	258(2)	543(1)	5.3(9)
C6	761(2)	295(1)	485(1)	4.2(7)
C7	710(3)	380(1)	490(2)	7.0(1)
O1	602(2)	321(2)	353(1)	6.8(7)
O2	667(2)	207(2)	298(1)	7.5(7)
C8	658(2)	261(2)	355(1)	4.8(8)
C9	600(3)	219(3)	226(2)	8.0(1)
C1p	768(2)	111(1)	727(1)	3.2(6)
C2p	769(2)	195(1)	743(2)	4.1(8)
C3p	811(2)	223(2)	813(1)	5.3(8)
C4p	849(2)	170(2)	872(1)	4.7(7)
C5p	848(3)	87(2)	858(2)	6.0(1)
C6p	810(3)	56(1)	783(1)	4.5(6)
C7p	825(2)	−6(2)	605(2)	5.1(9)
C8p	938(2)	4(2)	630(1)	4.6(8)
C9p	1010(2)	−50(2)	595(2)	6.0(1)
C10p	983(3)	−113(2)	544(2)	6.0(1)
C11p	877(3)	−114(2)	520(2)	5.3(9)
C12p	802(3)	−63(2)	546(2)	5.1(8)
C13p	593(2)	3(2)	652(2)	5.0(8)
C14p	616(2)	−75(1)	701(1)	4.4(8)
C15p	533(3)	−140(2)	697(2)	7.0(1)
C16p	412(3)	−103(2)	712(2)	8.0(1)
C17p	393(2)	−17(2)	664(2)	5.3(9)
C18p	483(2)	47(2)	673(2)	5.1(9)
C19p	480(2)	101(2)	746(1)	3.5(7)
C20p	378(2)	154(2)	748(2)	7.0(1)
C21p	494(4)	59(3)	825(2)	8.0(1)
C22p	531(4)	−181(2)	619(3)	10.0(1)
Om	434(4)	87(3)	307(3)	28.0(3)
Cm	382(6)	18(4)	318(4)	13.0(2)

e.s.d.'s were obtained by least-squares fitting of the θ-values of 24 intense reflections chosen from different regions of the reciprocal space in the range 20–25° using the Mo-K_{α_1} wavelengths (λ 0.709300 Å). The reflection intensities were corrected for Lorentz polarization and absorption effects by a ψ-scan method. The transmission factor was in the range 1.011–1.081.

The structure was solved by Patterson and Fourier techniques and refined by full matrix least-squares analysis by means of the SHELX 76 program [18]. The atomic scattering factors and anomalous scattering coefficients were taken from ref. 19. Calculations were carried out on the IBM 3031 computer of the Centro Nazionale Universitario di Calcolo Elettronico del C.N.R. (Pisa). Other programs used were PARST [20] and ORTEP [21]. The final atomic coordinates are shown in Table 3.

The difference Fourier map showed two connected peaks located around $0.40x$, $0.05y$, $0.31z$, which we believe to be due to a clathrate methanol molecule. In the final refinement cycles the scattering factor of the oxygen was assigned to the atom showing the lower thermal factor. Hydrogen atoms were introduced in calculated positions, with r(C–H) 1.01 Å *.

Acknowledgements

This work was carried out with support under the research program "Progetto Finalizzato per la Chimica Fine II".

References

1 B. Bosnich and M.D. Fryzuk, Topics Stereochem., 12 (1981) 119.
2 H. Brunner, Adv. Organomet. Chem., 18 (1980) 151.
3 T.C. Flood, Topics Stereochem., 12 (1981) 37.
4 S. Top, G. Jaouen, A. Vessieres, J-P. Abjean, D. Davoust, C.A. Rodger, B.G. Sayer and M.J. McGlinchey, Organometallics, 4 (1985) 2143, and ref. cited therein.
5 G. Jaouen in H. Alper (Ed.), Transition Metals in Organic Synthesis, Vol. 2, 1978, p. 65–180, Academic Press, New York.
6 K. Schlögl, Topics Curr. Chem., 125 (1984) 27.
7 P. Pertici, P. Salvadori, A. Biasci, G. Vitulli, M.A. Bennett and L.A.P. Kane-Maguire, J. Chem. Soc., Dalton Trans., (1988) 315.
8 G. Klopman and K. Noack, Inorg. Chem., 7 (1968) 579.
9 T.E. Sloan, Topics Stereochem., 12 (1981) 1.
10 M.A. Bennett, G.B. Robertson and A.K. Smith, J. Organomet. Chem., 43 (1972) C41.
11 K. Kan, Y. Kai, N. Yasuoka and N. Kasai, Bull. Chem. Soc. Jpn. 50 (1977) 1051; K. Kan, K. Miki, Y. Kai and N. Kasai, ibid., 51 (1978) 733.
12 P. Pertici, S. Bertozzi, R. Lazzaroni, G. Vitulli and M.A. Bennett, J. Organomet. Chem., 354 (1988) 117.
13 P. Pertici, G. Vitulli, R. Lazzaroni, P. Salvadori and P.L. Barili, J. Chem. Soc., Dalton Trans., (1982) 1019.
14 See for example: K. Schlögl, J. Organomet. Chem., 300 (1986) 219.
15 H. Brunner and R.G. Gastinger, J. Organomet. Chem., 145 (1978) 365.
16 D.F. Dersnah and M.C. Baird, J. Organomet. Chem., 127 (1977) C55.
17 F. Morandini, G. Consiglio, B. Straub, G. Ciani and A. Sironi, J. Chem. Soc., Dalton Trans., (1983) 2293.

* Lists of structure factors, thermal parameters and atomic coordinates for H atoms are available from the authors.

18 G.M. Sheldrick, SHELX 76, Program for Crystal Structure Determination, University of Cambridge, 1976.
19 International Tables for X-Ray Crystallography, Kynoch Press, Birmingham, 1974, Vol. 4.
20 M. Nardelli, Comput. Chem., 7 (1983) 95.
21 C.K. Johnson, ORTEP, Report ORNL 3794, Oak Ridge National Laboratory, Tennessee, 1965.